JOURNAL OF CATALYSIS 82, 332–340 (1983)

Electromotive-Forces Studies of Carbon Monoxide Oxidation on Platinum

HIROSHI OKAMOTO, GO KAWAMURA, AND TETSUICHI KUDO

Central Research Laboratory, Hitachi Ltd., 1-280, Higashi-Koigakubo, Kokubunji, Tokyo, Japan

Received March 9, 1982; revised July 14, 1982

The mechanism of CO oxidation on deposited Pt is analyzed by electromotive forces (emf) measurement for a solid electrolyte concentration cell where the partial pressures, P_{O_2} and P_{CO}, are between 5 Pa and 50 kPa, and the temperature range is 520 to 680°K. The emf is expressed as a function of the surface oxygen and CO concentrations adsorbed on Pt, with reasonable assumptions. Thus, emf dependence on P_{O_2} and P_{CO} shows surface species concentrations during reaction as functions of P_{O_2} and P_{CO}. As a result, in the region where CO is scarce compared to oxygen, surface CO concentration is determined to be proportional to $P_{O_2}{}^{\gamma}P_{CO}{}^{\delta}$, under the assumption that the surface oxygen concentration is constant. Here, δ is found to increase from 1 to about 1.6 with P_{CO}, γ is -1.4 at lower temperatures (about 580°K), and -1 at higher temperatures (about 670°K). This dependence is considered in terms of residence time and surface mobility for CO on Pt. In the region where CO is sufficient, the surface CO concentration is almost saturated and that of surface oxygen is expressed as $kP_{O_2}{}^{1.2}/P_{CO}{}^{1.1}$. Thus, CO oxidation in that case is considered to proceed with the rate-determining step of surface reaction between adsorbed CO and associatively adsorbed oxygen. The transient emf observed as P_{O_2} or P_{CO} increased or decreased stepwise also reveals that CO oxidation occurs via a Langmuir–Hinshelwood mechanism.

INTRODUCTION

The importance of measuring adsorption during surface catalysis has been emphasized by Tamaru (*1*). Adsorption measurement during CO oxidation on a Pt surface has been carried out by many investigators. At very low pressures between 10^{-6} and 10^{-3} Pa, surface oxygen has been determined by Auger electron spectroscopy (*2*) or by transient CO pressure-jump (*3, 4*), and surface CO by flash heating (*4, 5*). At high pressures of the order of 1 kPa, infrared spectroscopy has been employed for surface CO (*6–10*), and surface potential measurement for surface oxygen (*6*).

While these measurements were very enlightening, they did not clarify the amounts of surface oxygen and CO adsorbed during reaction as functions of P_{O_2} and P_{CO}. Ability to do this would permit reaction rates for CO oxidation to be explained in terms of the amounts of surface species.

The emf of solid electrolyte concentration cells with Pt electrodes of type

$$O_2(P_{O_2}) + CO(P_{CO}),\quad Pt/\text{stabilized } ZrO_2/Pt, O_2(P'_{O_2}), \quad (1)$$

has been shown to indicate surface adsorption states on Pt at low temperatures (about 600°K) (*8, 11, 12*). That is, the emf is generated by a mixed electrode potential involving electrochemical reactions of O^{2-} in stabilized ZrO_2 with the oxygen and CO adsorbed on Pt. Thus, it is known that if the progress of these electrochemical reactions is smaller than that of chemical oxidation on a Pt surface, the emf measurement is a high impedance probe into the surface adsorption states.

This paper clarifies the dependences of surface oxygen and CO concentrations adsorbed on Pt during reaction as functions of P_{O_2} and P_{CO}. To achieve this, emf measurement is employed along with some reasonable assumptions.

0021-9517/83 $3.00

METHODS

This section draws basic equations for the relations between emf and surface concentrations of adsorbed species, as well as between emf and partial pressures for reactant gases.

a. Assumptions

The emf, E, of solid electrolyte concentration cells (type (1)) deviates significantly at low temperatures around 600°K from that calculated using

$$E = (RT/4F)\ln (P'_{O_2}/P''_{O_2}), \qquad (2)$$

as shown in Fig. 1. Here, R is the molar gas constant, T the absolute temperature, F the Faraday constant, and P''_{O_2} the equilibrium O_2 partial pressure for the mixed gas of the reaction,

$$2CO + O_2 = 2CO_2. \qquad (3)$$

This is because reaction (3) on a mixed gas electrode is not in equilibrium but is stationary at low temperatures. Though oscillations in CO oxidation are often observed, they can also be thought of as multiple steady states (13–15).

The following assumptions are made to obtain relations between E and partial pressures or between E and surface concentrations of oxygen and CO on Pt, during reaction under steady states.

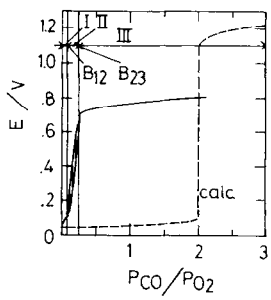

FIG. 1. E (emf) for a solid electrolyte concentration cell over the whole P_{CO} range with a fixed P_{O_2}. $O_2(P_{O_2})$ + $CO(P_{O_2})$, Pt/stabilized ZrO_2/Pt, $O_2(P'_{O_2})$, solid curve: observed emf, dashed curve: emf calculated from the Nernst Eq. (2), temperature: 613°K, P_{O_2}: 5 kPa, P'_{O_2}: 21 kPa.

(i) Surface oxygen on Pt during CO oxidation is either dissociatively or associatively adsorbed. Surface CO is associatively adsorbed.

(ii) Surface oxygen and CO concentrations adsorbed near a triple contact Pt-stabilized ZrO_2-gas, N_O (or N_{O_2}), and N_{CO}, respectively, are the same as those elsewhere on Pt.

(iii) N_O (or N_{O_2}) and N_{CO} are expressed as relations of the type:

$$N_O = g_O P_{O_2}{}^a P_{CO}{}^b, \qquad (4)$$

$$N_{O_2} = g_{O_2} P_{O_2}{}^{a'} P_{CO}{}^{b'} \qquad (5)$$

$$N_{CO} = g_{CO} P_{O_2}{}^c P_{CO}{}^d. \qquad (6)$$

Here, g_O, g_{O_2}, and g_{CO} are constants, while a, b, a', b', c, and d are parameters that are functions of P_{CO} and P_{O_2}.

(iv) Electrochemical reactions occur near a triple contact simultaneously with CO chemical oxidation on the whole Pt surface. The former do not disturb the latter.

(v) Electrochemical reactions involve two-electron reactions of surface oxygen and CO directly with O^{2-} ion in stabilized ZrO_2. These reactions bring about a mixed electrode potential, generating the observed emf.

Assumption (i) concerns oxygen and CO adsorption states during oxidation on Pt. Oxygen and CO adsorption species have been studied individually by many investigators (*4, 16–18*). In general, there is agreement that oxygen is dissociatively and CO is associatively adsorbed on Pt in the temperature region where oxidation occurs. Infrared spectroscopy has also established that CO is associatively adsorbed during oxidation (*6, 9, 12*). However, the oxygen adsorption state during oxidation is rather obscure. At very low pressures of the order of 10^{-4} Pa, dissociative adsorption has been assumed (*4, 13*). On the other hand, at high pressures of the order of 1 kPa, associative adsorption has often been assumed to explain rate equations (*7*). This paper treats the two adsorption states for oxygen separately.

Assumption (ii) is connected with assumption (iv). From these two assumptions N_O (or N_{O_2}) and N_{CO} represent the surface concentrations during oxidation regardless of the progress of electrochemical reactions. That is, the emf measurement is a high impedance probe into the surface adsorption states during chemical oxidation.

Assumption (v) is based on the results obtained by Okamoto *et al.* (*8, 12*). Although other electrochemical reactions may be possible, the two-electron reactions are postulated as operative. This assumption, together with assumptions (ii) and (iv), are now under investigation, though the latter two assumptions were indirectly checked previously (*12*).

Under these assumptions, E will be expressed as a function of surface oxygen and CO concentrations. If oxygen is adsorbed dissociatively, electrochemical reactions near a triple contact occur as:

$$O\sigma + 2e^- \rightleftarrows O^{2-} + \sigma \quad (7)$$

$$CO\sigma + O^{2-} \rightleftarrows CO_2 + \sigma + 2e^- \quad (8)$$

Here, $O\sigma$, etc., denote oxygen, etc., adsorbed on Pt; e^- is an electron in Pt; and σ is a vacant site on Pt. If oxygen is adsorbed associatively, reaction (7) follows an additional electrochemical reaction:

$$O_{2-\sigma} + 2e^- \rightleftarrows O^{2-} + O\sigma \quad (9)$$

b. Basic Equations for Dissociative Oxygen Adsorption

An expression for E will first be obtained for the case of dissociative oxygen adsorption. Because current is not taken from the cell system, the rate differences between forward and backward reactions for reactions (7) and (8) are the same:

$$k_7 N_O \exp(2\alpha_{k_7} FE_m/-RT) - k_{-7} N_\sigma \exp(2\alpha_{a_7} FE_m/RT) = k_8 N_{CO} \exp(2\alpha_{a_8} FE_m/RT) - k_{-8} N_\sigma P_{CO_2} \exp(2\alpha_{k_8} FE_m/-RT). \quad (10)$$

Here, k_7, k_{-7}, k_8, and k_{-8} are forward and backward rate constants for reactions (7) and (8), α_k, α_a are cathodic and anodic charge transfer coefficients, E_m is a mixed electrode potential relative to the potential in the absence of CO.

The standard reversible potential for reaction (8) is about 1.2 V, so the backward reaction can be ignored. If experiments are carried out with FE_m/RT less than -1, the backward reaction for reaction (7) can also be ignored. Since α_k and α_a are generally about 0.5, Eq. (10) is simplified approximately as:

$$k_7 N_O \exp(FE_m/-RT) = k_8 N_{CO} \exp(FE_m/RT). \quad (11)$$

Thus,

$$E_m = (RT/2F)\ln(k_7 N_O/k_8 N_{CO}). \quad (12)$$

Using:

$$E = -E_m + E_r, \quad (13)$$

where E_r is a reference electrode potential relative to the mixed gas electrode potential in the absence of CO, E is expressed as:

$$E = (RT/2F)\ln(k_8 N_{CO}/k_7 N_O) + E_r. \quad (14)$$

This is the basic E and N_{CO}/N_O equation for dissociative adsorption of oxygen.

c. Equations for Constant N_O or N_{CO}

If N_O is independent of P_{O_2} and P_{CO}, Eq. (14) can be reduced to:

$$E = (RT/2F)\ln N_{CO} + G_1, \quad (15)$$

where G_1 is a constant. Using Eq. (6),

$$E = (RT/2F)\ln(P_{O_2}{}^c P_{CO}{}^d) + G_1', \quad (16)$$

where G_1' is a constant. Parameters c and d are determined by experiments using the following:

$$c = (2F/2.3RT)\partial E/\partial \log P_{O_2}|_{P_{CO}} \quad (17)$$

$$d = (2F/2.3RT)\partial E/\partial \log P_{CO}|_{P_{O_2}}. \quad (18)$$

With parameters c and d, N_{CO} can be expressed as a function of P_{O_2} and P_{CO}.

On the other hand, if N_{CO} is independent of P_{O_2} and P_{CO}, the same process can be applied, yielding:

$$E = (-RT/2F)\ln N_O + G_2, \quad (19)$$

$$a = (-2F/2.3RT)\partial E/\partial \log P_{O_2}|_{P_{CO}} \quad (20)$$

$$b = (-2F/2.3RT)\partial E/\partial \log P_{CO}|_{P_{O_2}}. \quad (21)$$

Here, again, G_2 is a constant. With parameters a and b, N_O can be expressed as a function of P_{O_2} and P_{CO}. It should be pointed out that the difference in E is more important than the absolute value of E in determining parameters a, b, c, and d.

d. Equations for Associative Oxygen Adsorption

Now, E will be expressed for the case of associative oxygen adsorption. In this case, the equations are somewhat complex. At the steady state the following equations can be approximately written, ignoring backward reactions:

$$k_9 N_{O_2} \exp(2\alpha_{k_9} F E_m/-RT) + k_7 N_O \exp(2\alpha_{k_7} F E_m/-RT) = 2k_8 N_{CO} \exp(2\alpha_{a_8} F E_m/RT), \quad (22)$$

$$k_9 N_{O_2} \exp(2\alpha_{k_9} F E_m/-RT) = k_7 N_O \exp(2\alpha_{k_7} F E_m/-RT). \quad (23)$$

Since charge transfer coefficients are near 0.5, E_m is expressed as:

$$E_m = (RT/2F)\ln(k_9 N_{O_2}/k_8 N_{CO}). \quad (24)$$

Taking relation (13) into consideration, E is described as:

$$E = (RT/2F)\ln(k_8 N_{CO}/k_9 N_{O_2}) + E_r. \quad (25)$$

This relation is the same as Eq. (14), except for constants. Thus, N_{O_2} and N_{CO} can be determined in the same way as described above. If reaction (7) is slower than reaction (9), at the steady state,

$$N_O > N_{O_2}. \quad (26)$$

As N_O is negligible relative to N_{O_2} on the Pt surface from the assumption, this relation near a triple contact may disturb chemical oxidation. Therefore, reaction (7) is not considered slower than reaction (9).

e. Experimental Methods

Preparations for solid electrolyte concentration cells and experimental apparatus were the same as described previously (*12*), so only a brief description will be presented here.

A Y_2O_3 (8 mol%)-stabilized ZrO_2 sintered pellet was used as a solid electrolyte, with a diameter and thickness of about 20 and 1 mm, respectively. Pt electrodes were deposited by electron-beam evaporation with a 0.1-μm thickness, and 12 mm diameter.

A block diagram of the emf measurement is shown in Fig. 2. All gases were commercially available types. These gases were appropriately mixed with the aid of a thermal mass flow control system. The emf was recorded via an impedance converter by recorder in parallel with Pt surface temperature.

RESULTS

a. E Over the Whole P_{CO} Range

E over a wide P_{CO} range has been described elsewhere (*12*), so only a brief description will be presented here. Over a certain P_{CO} range at a fixed P_{O_2}, E oscillates as shown in Fig. 1. This region is called region II, and those for lower and higher P_{CO}, region I and region III, respectively. The boundary between regions I and II is labeled B_{12}, that between regions II and III, B_{23}.

b. Transient E

The E change against time when P_{CO} is increased stepwise with a fixed P_{O_2} = 10

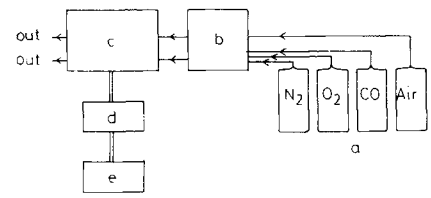

FIG. 2. Block diagram for emf measurements. a, Gas cylinders; b, thermal mass-flow control system; c, oxygen sensor setup; d, impedance converter; e, recorder.

kPa at T_0 (surface temperature in the absence of CO) = 568°K in regions I and II is shown in Fig. 3. Stepwise increase in P_{CO} from 0.05 to 0.1 kPa results in a slow E increase. However, when P_{CO} is increased from 0.1 to 0.2 kPa, E increases rapidly and sharply. A further increase from 0.2 to 0.3 kPa causes E to overshoot, i.e., to be temporarily more than the stationary value. After several tens of seconds E settles to the stationary value. This tendency becomes significant with further increases in P_{CO}. Moreover, E begins to oscillate. For P_{CO} = 0.4 kPa, the oscillation amplitude is very small and its regularity is low. However, a further increase in P_{CO} from 0.4 to 0.6 kPa brings about a clear oscillation in E accompanied with overshooting.

This overshooting phenomenon in E was observed even when P_{CO} was increased as slowly as possible. Experiments under opposite conditions where P_{O_2} was decreased with a fixed P_{CO} showed a similar tendency.

The change of E against time when P_{CO} is decreased stepwise with a fixed P_{O_2} = 10 kPa at T_0 = 571°K in regions III and II is shown in Fig. 4. When P_{CO} is decreased from 2.8 to 2.0 kPa, E decreases sharply and rapidly. A further decrease in P_{CO} from 2.0 to 1.15 kPa induces E to be temporarily less than the stationary value. After several minutes E approaches the stationary value. This tendency becomes significant with a decrease from 1.15 to 1.0 kPa. The surface temperature increase was less than 2°K for P_{CO} higher than 1 kPa.

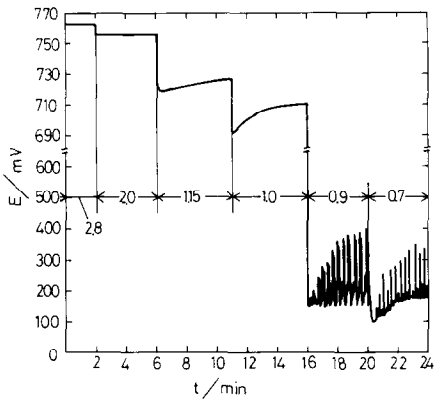

FIG. 4. Transient E in regions III and II with a fixed P_{O_2}. P_{O_2}: 10 kPa, T_0: 571°K, values in the figure: P_{CO} (kPa).

However, a decrease from 1.0 to 0.9 kPa brings about a great decrease in E and an oscillation with overshooting. At the same time, an abrupt surface temperature increase was observed up to 7°K which then dropped slowly to 5°K. Further decreases in P_{CO} induce oscillations with smaller amplitudes, accompanied by overshooting phenomena.

c. *E versus log P*

The relation between E and log P_{CO} in region I with a fixed P_{O_2} = 0.5 kPa at T_0 = 578°K is shown in Fig. 5. In this run, the

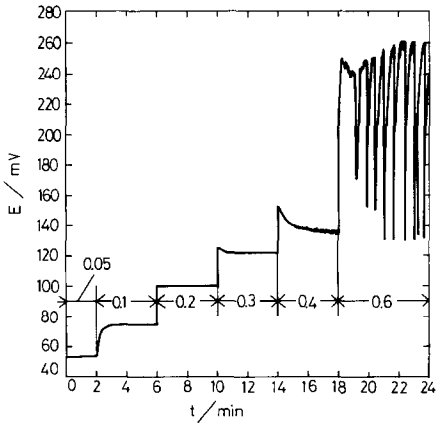

FIG. 3. Transient E in regions I and II with a fixed P_{O_2}. P_{O_2}: 10 kPa, T_0 (surface temperature in absence of CO): 568°K, values in the figure: P_{CO} (kPa).

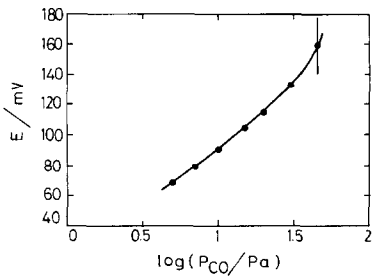

FIG. 5. Relation between E and log P_{CO} in region I with a fixed P_{O_2}. P_{O_2}: 0.5 kPa, T_0; 578 $K(RT_0/F$ = 50 mV), E_r (E in absence of CO): 20 mV.

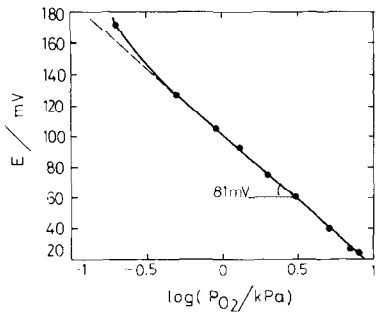

FIG. 6. Relation between E and log P_{O_2} in region I with a fixed P_{CO}. P_{CO}: 20 Pa, T_0: 578°K.

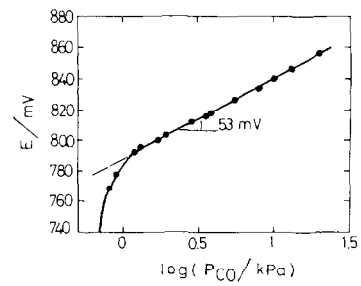

FIG. 7. Relation between E and log P_{CO} in region III with a fixed P_{O_2}, P_{O_2}: 4.6 kPa, T_0: 574°K.

surface temperature increase was less than 0.5°K, so these plots were isothermal. The value of RT/F is 50 mV, and E_r (E in the absence of CO) was 20 mV. Therefore for E above 70 mV, Eq. (18) is operative, if N_O (or N_{O_2}) is constant in region I. The slope of E against log P_{CO}, $2.3dRT/2F$, shows a gradual increase. That is, d increases from 1 to about 1.6.

The relation between E and P_{O_2} in region I with a fixed P_{CO} = 20 Pa at T_0 = 578°K is shown in Fig. 6. No surface temperature increase was observed in this run. All E values in this figure were RT/F (50 mV) greater than E_r. Therefore, if N_O (or N_{O_2}) is constant, Eq. (17) is operative. The slope of E against log P_{O_2} is about 81 mV, i.e., c equals -1.4 at P_{O_2} above 0.5 kPa. In the absence of CO, the slope was 29 mV, which equals the calculated value, $2.3RT/4F$ (Eq. (2)). At higher temperatures, such as 670°K, c was about one.

The relation between E and log P_{CO} in region III with a fixed P_{O_2} = 4.6 kPa at T_0 = 574°K is shown in Fig. 7. All E values in this figure are RT/F (49 mV) greater than E_r. As N_{CO} is almost constant in region III (*8, 12*), Eq. (21) is operative. The slope of E against log P_{CO} is about 53 mV, showing that b (or b') is -1.1 for P_{CO} above 1 kPa. For P_{CO} less than 1 kPa, the slope increases and oscillation occurs as P_{CO} is decreased. The Pt surface temperature was almost constant for P_{CO} above 1 kPa.

The relation between E and log P_{O_2} in region III with a fixed P_{CO} = 2 kPa at T_0 = 571°K is shown in Fig. 8. As with Fig. 7, all E values in this figure are RT/F greater than E_r and Eq. (20) is operative. The slope of E against log P_{O_2} is 62 mV, meaning that a (or a') is 1.2, for P_{O_2} below 4 kPa. For P_{O_2} above 4 kPa, the slope increases and oscillations begin as P_{O_2} is increased. The surface temperature increase was almost linear with P_{O_2} within 1°K, until oscillations occurred.

Parameters a, b (or a', b'), c, and d determined as above at about 580°K, with estimated values in region II where stationary E could not be obtained, are shown in Fig. 9. In region I, it is postulated that N_O (or N_{O_2}) is constant, expressed as:

$$N_O \text{ (or } N_{O_2})(\text{I}) \propto P_{O_2}{}^0 P_{CO}{}^0. \qquad (27)$$

N_{CO} can be written as:

$$N_{CO}(\text{I}) \propto P_{CO}{}^{\delta}/P_{O_2}{}^{1.4}, \qquad (28)$$

where δ increases from 1 to about 1.6 as P_{CO} is increased. The order of P_{O_2} ap-

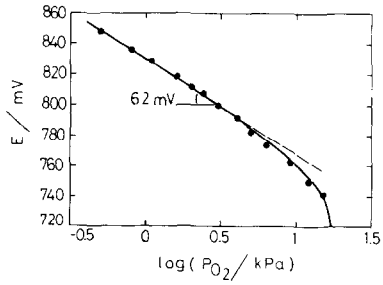

FIG. 8. Relation between E and log P_{O_2} in region III with a fixed P_{CO}. P_{CO}: 2 kPa, T_0: 571°K.

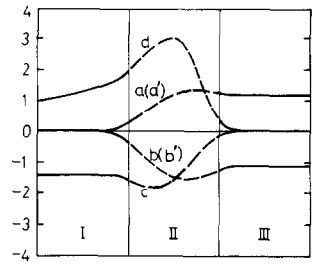

FIG. 9. Parameters a, b (or a', b'), c, and d for each region. $N_O = g_O P_{O_2}{}^a P_{CO}{}^b$, $N_{O_2} = g_{O_2} P_{O_2}{}^{a'} P_{CO}{}^{b'}$, $N_{CO} = g_{CO} P_{O_2}{}^c P_{CO}{}^d$, N_O, etc.: surface oxygen, etc., concentrations on Pt, g_O, etc.: constants, T_0: about 580°K.

proached 1 as temperature increased to about 670°K. In region III, N_{CO} is constant, indicating:

$$N_{CO}(\text{III}) \propto P_{O_2}{}^0 P_{CO}{}^0. \tag{29}$$

N_O (or N_{O_2}) has the form:

$$N_O \text{ (or } N_{O_2})(\text{III}) \propto P_{O_2}{}^{1.2}/P_{CO}{}^{1.1}. \tag{30}$$

Near B_{23} in region III, the expression N_O (or N_{O2}) was somewhat ambiguous because isothermal plots were not obtained. However, it seemed that b became smaller than -1.1 and a greater than $+1.2$.

DISCUSSION

Surface adsorption states on Pt during CO oxidation will be discussed in connection with the kinetics.

a. N_O (or N_{O_2}) and N_{CO} Over the Whole Range of Gas Compositions

First, N_O (or N_{O_2}) and N_{CO} will be looked at roughly, then discussed for regions I and III in detail. The N_O (or N_{O_2}) and N_{CO} variation over the whole gas composition range is shown in Fig. 10. This figure is based on results obtained here as well as those reported in the literature (*8, 9, 12*).

In region I, the surface oxygen concentration is assumed to be almost constant. Surface CO is also present but the amount is very small (*8, 12*). In region II, most surface oxygen is replaced by surface CO. The N_{CO} increase is steeper than the N_O decrease indicated by Fig. 9. In region III, surface CO is saturated (*8, 12*), and N_O (or N_{O_2}) is very small. The N_{CO} there is larger than N_O in region I (*9*). This illustration is consistent with results obtained by Golchet and White (*4*) and Matsushima (*5*). Over the whole gas composition range, the reaction is thought to proceed via a Langmuir–Hinshelwood mechanism including the surface reaction of the adsorbed species (*5, 12, 20*); this will be confirmed below.

b. Region I

The value of N_{CO} is given by Eq. (28) where the order of P_{O_2} was 1.4 at 578°K under the assumption that N_O is constant. This value is not easy to explain in terms of the simple Langmuir–Hinshelwood mechanism. If the reaction proceeds via the simple Langmuir–Hinshelwood mechanism,

$$CO + \sigma \rightarrow CO\sigma, \tag{31}$$

$$O_2 + 2\sigma \rightarrow 2O\sigma, \tag{32}$$

$$CO\sigma + O\sigma \rightarrow CO_2 + 2\sigma, \tag{33}$$

then the reaction rate, v(I) is expressed by

$$v(\text{I}) \propto N_{CO} N_O. \tag{34}$$

Here, oxygen adsorption is considered to be dissociative. This is because in region I the surface CO concentration is so small that the reaction system can be approximately regarded as that of oxygen-Pt, where it is established that oxygen adsorbs dissociatively (*4, 16–18*). Since v(I) is determined experimentally (*12*) as

$$v(\text{I}) \propto P_{CO}, \tag{35}$$

N_O can be calculated using Eq. (28),

$$N_O \propto P_{O_2}{}^{1.4}/P_{CO}{}^{\delta-1}. \tag{36}$$

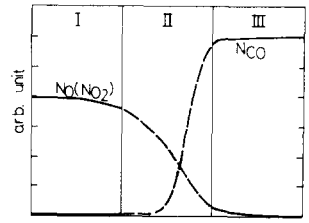

FIG. 10. Schematic diagram for N_O (or N_{O_2}) and N_{CO}. T_0: about 580°K.

This N_O expression is in conflict with the assumption that N_O is constant. Therefore, Eq. (28) should be explained in terms of a modified Langmuir–Hinshelwood mechanism.

Equation (35) shows that CO-supply is a rate-determining step. Therefore, N_{CO} should be interpreted in terms of residence time for CO on the Pt surface. Oxygen adsorption on Pt is almost saturated in region I, while many vacant sites remain for CO (*9*). Once CO is adsorbed on the Pt surface, it will either react readily with neighboring oxygen or move until it encounters an adsorbed oxygen where it reacts if CO is adsorbed in the midst of vacant sites. The residence time for CO on the Pt surface for the former case is near zero and that for the latter case has some positive value.

If adsorbed CO mobility is sufficiently high on Pt, then N_{CO} should be nearly zero and independent of P_{O_2}, because of the near saturation adsorption of oxygen. If adsorbed CO mobility is low, N_{CO} depends on P_{O_2} for the following reason. Oxygen is in dynamic adsorption–desorption equilibrium and gaseous oxygen can be adsorbed to the adjacent adsorbed CO, accompanied with oxygen desorption from another site. Then, the adjacent adsorbed CO and oxygen readily react and the CO residence time reduces. This possibility increases as P_{O_2} increases.

Thus, the order of P_{O_2} in N_{CO} can be interpreted in terms of adsorbed CO mobility. This interpretation is consistent with the fact that the P_{O_2} dependence of N_{CO} decreased as temperature increased. On the other hand, the order of P_{CO} in N_{CO} increased from 1 to 1.6 as P_{CO} was increased. This result seems to be related to E oscillation because N_{CO} varied substantially when P_{CO} was varied a little near B_{12}.

As gas composition approached that for region II, E overshot when P_{CO} was increased stepwise (Fig. 3). This indicates that N_{CO} was temporarily greater or N_O was temporarily less than that for a following stationary state. That is, the surface reaction cannot keep up with the gaseous composition change. This implies that the distribution of oxygen and CO adsorbed on Pt changes. Therefore, the rate-determining step moves from CO-supply to surface reaction between adsorbed species, with experimental conditions approaching those in region II. These phenomena are evidence of a Langmuir–Hinshelwood mechanism.

c. Region III

Although the discussion of the surface adsorption states in region I was rather speculative, that for region III is lucid. The N_O (or N_{O_2}) in region III was expressed by Eq. (30). This equation implies two things. One is that the Pt surface is almost covered with CO, since the order of P_{CO} is close to -1. This is consistent with N_{CO} being constant.

The other is that oxygen is associatively adsorbed, i.e., N_{O_2} is a more appropriate expression than N_O. This is because, otherwise, N_O should be proportional to $P_{O_2}^{0.5}/P_{CO}$ in view of the competitive adsorption equilibrium where CO is almost saturated. This adsorption equilibrium is established in region III, or in the presence of sufficient oxygen and CO with low oxidation rates. Although oxygen is often thought to be dissociatively adsorbed even during reaction (*16*), Eq. (30) shows that oxygen adsorbed on Pt is actually molecular under working conditions in region III.

The reaction rate in region III, v(III), was given as (*8, 12*):

$$v(\text{III}) = k(\text{III})P_{O_2}/P_{CO}. \tag{37}$$

This equation combined with Eqs. (29) and (30) reveals elementary steps for CO oxidation in the following manner:

$$O_2 + \sigma \rightleftarrows O_{2-\sigma} \tag{38}$$

$$CO + \sigma \rightleftarrows CO\sigma \tag{39}$$

$$O_{2-\sigma} + CO_\sigma \rightarrow CO_2 + O_\sigma + \sigma \tag{40}$$

$$CO_\sigma + O\sigma \rightarrow CO_2 + \sigma. \tag{41}$$

These steps were proposed earlier by Coch-

ran *et al.* (*7*), and are confirmed here by determining N_O (or N_{O_2}) and N_{CO} during reaction. If reaction (40) is a rate-determining step and reaction (41) is fast, then the reaction rate is expressed as:

$$v(\text{III}) \propto N_{O_2} N_{CO}. \tag{42}$$

Using Eqs. (29) and (30),

$$v(\text{III}) \propto P_{O_2}^{1.2} / P_{CO}^{1.1}. \tag{43}$$

This is almost the same as Eq. (37).

CONCLUSIONS

It has been shown that emf is very useful in the study of surface adsorption states under working conditions. The method has been applied to CO oxidation on Pt and has revealed that the surface oxygen and CO concentrations can be determined as functions of P_{O_2} and P_{CO} with suitable assumptions. With these results, the mechanism of CO oxidation on Pt has been clarified and specifically discussed in terms of surface adsorption states.

REFERENCES

1. Tamaru, K., *Adv. Catal.* **15,** 65 (1964).
2. Hopster, H., Ibach, H., and Comsa, G., *J. Catal.* **46,** 37 (1977).
3. White, J. M., and Golchet, A., *J. Chem. Phys.* **66,** 5744 (1977).
4. Golchet, A., and White, J. M., *J. Catal.* **53,** 266 (1978).
5. Matsushima, T., *Bull. Chem. Soc. Jpn.* **51,** 1956 (1978).
6. Heyne, H., and Tompkins, F. C., *Proc. Roy. Soc. London* **292,** 460 (1966).
7. Cochran, H. D., Donnelly, R. G., Modell, M., and Baddour, R. F., *Colloid Interface Sci.* **3,** 131 (1976).
8. Okamoto, H., Obayashi, H., and Kudo, T., *Solid State Ionics* **3/4,** 453 (1981).
9. Shigeishi, R. A., and King, D. A., *Surf. Sci.* **75,** L397 (1978).
10. Cant, N. W., and Donaldson, R. A., *J. Catal.* **71,** 320 (1981).
11. Okamoto, H., Obayashi, H., and Kudo, T., *Solid State Ionics* **1,** 319 (1980).
12. Okamoto, H., Kawamura, G., and Kudo, T., *J. Catal.* **82,** 322 (1983).
13. Turner, J. E., Sales, B. C., and Maple, M. B., *Surf. Sci.* **103,** 54 (1981).
14. Bykov, V. I., Yablonskii, G. S., and Elokhin, V. I., *Surf. Sci.* **107,** L334 (1981).
15. Takoudis, C. G., Schmidt, L. D., and Aris, R., *Surf. Sci.* **105,** 325 (1981).
16. Engel, T., and Ertl, G., *Adv. Catal.* **28,** 1 (1979).
17. Gland, J. L., *Surf. Sci.* **93,** 487 (1980).
18. Gland, J. L., Sexton, B. A., and Fisher, G. B., *Surf. Sci.* **95,** 587 (1980).